# Compensation Network Design for Capacitive Ultrasonic Transducers

**S.G. Mc Sweeney, W.M.D. Wright**

*Department of Electrical Engineering,*

*University College Cork*

*Abstract*— **The frequency response characteristic of a through transmission Capacitive Ultrasonic Transducer (CUT) system is quite often dominated by membrane resonances of the transmit and receive devices and transmission channel distortion. Simple analog filtering stages may be appropriately designed to compensate for the most pronounced of these channel effects. In many ultrasonic inspection applications a reasonable SNR of the received signal across the passband is important since frequency dependant attenuation is being measured. The design and simulation of Zobel T, lattice, and biquadratic op amp cascaded equalisation filter architectures to address this issue are presented in this work.**

*Keywords* – **Capacitive Ultrasonic Transducers, Zobel, Optimisation**

## I INTRODUCTION

Capacitive ultrasonic transducers (CUTs) [1-3] and capacitive micromachined ultrasonic transducers (cMUTs) [4-7] are well-established technologies and are finding increasing application in medical and industrial measurement. Whilst their performance in air is generally superior to that of most piezoelectric devices, membrane resonance still presents an issue where thicker membranes are required for more rugged devices. Hence, both air-coupled and immersion devices could benefit significantly by bandwidth and resonance modification through the use of selective networks. By manipulating the poles/zeroes of a filtering circuit, the transmission characteristics can be modified to enhance transducer performance. One of the advantages for CUTs and cMUTs is that variations in transducer performance, produced by any lack of repeatability in their manufacture, may be reduced to a level that has a negligible affect on the key response characteristics of the system. For cMUTs, an additional advantage is that the selective network may be incorporated with the transducer on a suitable BiCMOS-compatible IC.

The use of front end mounted components in CUTs and cMUTs is not a new concept, filter networks have been tightly integrated into capacitive sensing and transmission devices by a number of groups. Among other methods, flip chip bonding has been used to integrate cMUT arrays with ASIC designs. Resonator circuits are widely employed in EMRF (Electromagnetic Radio Frequency) transmission and receive systems including among others passive, cascode active and cascade active selective designs. Selective networks allow for maximising the excitation signal of a sensor off resonance [8], assuming that a physical limit of the sensor is not exceeded (dielectric strength, membrane stress, collapse force etc.). The frequency response of the sensor when viewed from outside the network is modified. Such conditioning comes at the expense of power consumption, phase distortion, non-linearity or reduced SNR (signal to noise ratio) or some combination of these effects.

The bandwidth of an ultrasonic system can most practically be defined as the transmission envelope of a transmitter/receiver pair. In many ultrasonic through transmission systems, this is a critical parameter as the frequency response data is being measured, from which information about the medium or media that the ultrasonic wave passed through can be derived. The greater the bandwidth the greater the ability of the system to interrogate a wider range of phenomena along its path. Additionally, in many of these systems, the impulse response settling time becomes critical as typically an array of these devices are time multiplexed and the shorter the impulse response time of a single device, the greater the scanning system refresh rate.

In air, a transmitter will typically be designed to be highly resonant in order to maximise range or sensitivity, however a receiver should inherently have a wider bandwidth as the thinner membrane dominates the oscillations to a lesser extent. At close range, the additional transmit power afforded it by a

resonant design is unnecessary and any extra bandwidth on the transmission end of such a system can have significant impact on the overall sensor resolution. In the early days of the telecommunications industry, when Electromagnetic (EM) transmission lines used analog communication methods, a similar problem was encountered with frequency dependant attenuation that was complex and required composite filtering in order to maintain low signal error rates. This difficulty was solved with the use of Zobel networks [9], which were developed using the image impedance method. The aim of this work is to apply the methodology used by Zobel for EM transmission lines to acoustic transmission lines to give superior performance characteristics.

The CUT and cMUT, having evolved from the electret condenser microphone, share a number of similarities with their ancestor. One of the most important of these is the significant DC pull in voltage required to establish ultrasonic transmission. Consequentially, the AC signal carrier represents a small percentage of the overall voltage and as such amplification in the order of 6dB in most devices will not result in corona discharge from dielectric breakdown. Thus, this gives significant freedom to modify the AC signal to a transmitter to enhance bandwidth and settling time among other parameters as long as care is taken not to exceed 6dB in increased transmitter driving voltage amplitude.

Section II outlines the system model developed for simulation purposes, Section III will describe the design and simulation of the various networks used in this work, Section IV will give conclusions from this work.

## II SYSTEM MODELLING

A lumped element electrical equivalent model as outlined in [10] was developed for the transmitting and receiving CUT mechanical and electrical dynamics. An illustrative diagram of the system in its most basic form may be seen in Figure 1. For the purposes of the modelling conducted, the decoupling dynamics have been assumed ideal (all pass in magnitude and phase). Additionally, the source and sink are assumed ideal and as such are not modelled. From the model for a transmitting CUT as developed by [11], which incorporates the phenomenon of spring softening, the transmit side transfer function may be defined in the frequency domain by equation 1:

$$G_{Tx}=\frac{(C_{0T}C_{mT}R_{rT}s)}{(C_{0T}-C_{mT}+C_{0T}C_{mT}(R_{dT}+R_{rT})s+C_{0T}C_{mT}L_{mT}s^2)} \quad (1)$$

where $C_{0T}$ is the transmitter electrical capacitance, $C_{mT}$ is the mechanical capacitance, $R_{rT}$ is the radiation resistance, $L_{mT}$ is the mechanical inductance and $R_{dT}$ is the dissipation resistance which

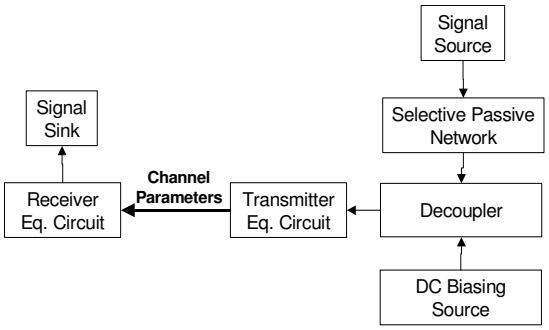


**Figure 1: System Diagram**

approximates the losses in the device. These properties in themselves have complex derivations due to the lack of measurable data the background of which can be found in [12].

The acoustic channel attenuation in air is appropriately captured by the work of Bond [13] using the molecular model derivation. This attenuation coefficient is suitable for the hundreds of kHz operating range and may be given by equation 2 for transmission in air:

$$\alpha=\frac{15.895x10^{-11}\sqrt{\frac{T_0}{T_{ref}}}}{p_0/p_{ref}}f^2 \quad (2)$$

where $\alpha$ is the attenuation coefficient in dB/m, $T_0$ is the current temperature, $T_{ref}$ is the reference temperature, $p_0$ is the current pressure and $p_{ref}$ is the reference pressure. The voltage across the electroacoustically transformed equivalent radiation resistance ($V_{rT}$) can then be related to pressure along the acoustic axis $p(r)$, at a distance $r$, within air of density $\rho_o$, from a circular membrane of area $S_T$, vibrating at a frequency $f$ by equation 3:

$$p(r)=\frac{j\rho_0 f S_T V_{rT}}{\varphi_T r R_{rT}} \quad (3)$$

where $j = \sqrt{-1}$ and $\varphi_T$ is the electroacoustic transformation factor for the transmitter. Additionally, the responsiveness of the receiver CUT membrane in the electrical domain to its incident pressure ($p(r)$) may be given as a function of its electroacoustic transformation factor $\varphi_R$ and membrane surface area $S_R$ by equation 4:

$$V_{rR}=\frac{2p(r)S_R}{\varphi_R} \quad (4)$$

Consequentially the transfer function in the frequency domain for the acoustic channel may be given by equation 5:

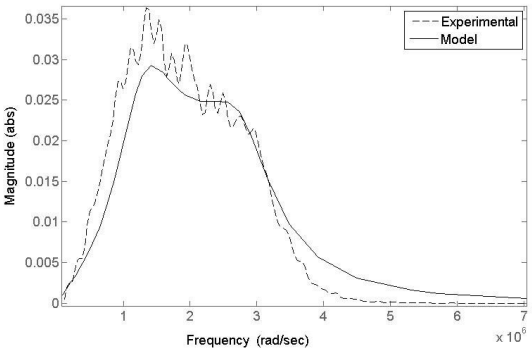


**Figure 2: System Magnitude Response Envelope**

$$G_{AC} = \left( \frac{s\rho_0 S_T S_R}{\pi r R_{rR} \varphi_T \varphi_R} \right) 10^{\frac{7.947x10^{-12} s^2 p_{ref} r \sqrt{T_0/T_{ref}}}{(2\pi)^2 p_0}} \quad (5)$$

The transfer function for the receiver CUT incorporating spring softening, in which the driving voltage is related to the incident pressure, as described in equation 4, may be given by equation 6:

$$G_{Rx} = \frac{1}{C_{0R}\left( L_{mR}s^2 + (R_{dR} + R_{rR})s + 1/C_{mR} \right)} \quad (6)$$

where the subscript *R* denotes the receiver parameters as defined for equation 1. The overall system response ($G_{sys}$) may then be simply defined as the product of the transfer functions. In order to give a concrete indication of the direct applicability of this work, numerical model parameters were used that match those of a system from which frequency response data was obtained. The experimentally obtained and modelled magnitude response plots of the system used in this work are overlaid in Figure 2. As can be seen there is reasonable model fidelity. The variation in modelled and experimentally obtained data may be explained by an additional frequency dependant effect that is not being captured in the lumped element model.

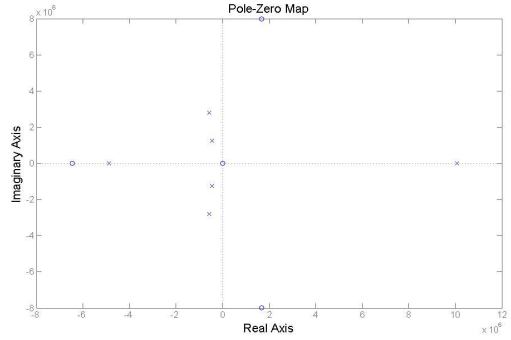


**Figure 3: Pole-Zero Map of Model**

From Figure 2, it is evident that all of the required dynamics of the system have been captured for the purposes of this work. It should be noted that experimentally obtained impulse response data was also analysed and correlated with the model.

## III COMPENSATION NETWORK DESIGN

In order to locate the system poles and zeros, a Pade approximation was performed on the acoustic channel transfer function. This approximation was performed to a numerator of 3 and a denominator of 4 about the centre frequency of 300kHz. The resulting pole-zero plot of the system is shown in Figure 3.

As mentioned previously, the identified optimisation parameters are the system bandwidth and the impulse response settling time. Additionally, reductions in system sensitivity below 3dB cannot be tolerated usually in air coupled ultrasonic systems due to the low SNR resulting from the high reflection coefficient encountered at solid-gas interfaces.

### *a) Passive Design*

The first design approach adopted was that of passive equalization filtering. A passive design approach was adopted, as opposed to active or digital as typically ultrasonic transducers are used in conjunction with sophisticated rf pulser systems that have peak pulse voltages in the region of 100s of volts and typically pulse shaping requires a linear amplifier which introduces significant cost and complexity into the ultrasonic system.

Zobel T and lattice networks were used in the design of the passive compensation network whose basic structure may be seen in Figure 4(a). These networks were selected for very specific reasons. The Zobel T network has a constant input and output impedance across the frequency domain. Consequently, this network is ideally suited to passive magnitude equalisation designs that require a number of degrees of freedom as the parameter dependence of neighbouring sections can be decoupled. The Lattice Zobel (Figure 4(b)) network comes into its own in the field of passive phase equalisation as it presents a constant resistance and is intrinsically balanced due to its architecture.

In this work only one particular architecture of the Zobel T network was used, the bandpass section. This restriction was to reduce the level of

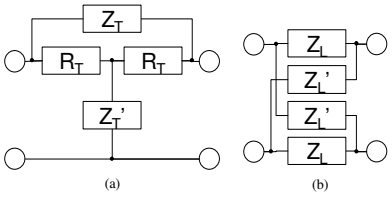


**Figure 4: Zobel T (a) and Lattice (b) Structures**

design flexibility and thus the complexity of the formulae required to obtain equation 12 and equation 13. The transfer function for a single Zobel T section is given by equation 7:

$$G_T = \frac{1/Z_T + \dfrac{R_T Z_T'}{R_T + Z_T' + R_0^2 Z_T'}}{1/Z_0 + 1/Z_T + \dfrac{R_T + Z_T'}{R_T Z_T'}} \tag{7}$$

where $R_0$ is the matching impedance, $Z_T$ and $Z_T$' are the series and dual impedances of the Zobel section respectively. As can be observed, there is a dependency of the section on the load impedance. However, this can be controlled in all but the first section of a cascaded filter design. The Lattice phase equaliser section (as with the Zobel T section) was restricted to a single architecture. From observation of the phase response of the unmodified system it is evident that this system would benefit from phase equalisation, which would result in shorter settling times. The transfer function for a single Lattice Zobel section is given by equation 8 and equation 9:

$$G_L = \frac{Z_0 - Z_L}{Z_0 + Z_L} \tag{8}$$

$$Z_0^2 = Z_L Z_L' \tag{9}$$

where $Z_0$ is the terminating impedance of the lattice section and $Z_L$ and $Z_L$' are the lattice section series and dual impedances. The passive equalisation network developed was limited to two T bridge and two Lattice Zobel networks in order to limit complexity. The overall transfer function may thus be defined by equation 10:

$$G = G_{sys} G_{T1} G_{T2} G_{L1} G_{L2} \tag{10}$$

where $G_{L1}$ and $G_{L2}$ are the first and second lattice section transfer functions and $G_{T1}$ and $G_{T2}$ are the first and second T section transfer functions . These transfer functions will differ significantly due to the differing loading impedance observed which for accurate results must be incorporated into the transfer function itself. The first of the critical parameters to optimise is only affected by the T bridge sections of the design as the lattice sections only provide a phase shift. Hence, the 3dB bandwidth may be simply defined by equation 11:

$$\beta = \alpha_H - \alpha_L \tag{11}$$

where $\alpha_H$ and $\alpha_L$ are the positive real roots of the magnitude of the transfer function defined in equation 10 for the variables in equations 1, 6 and the Pade approximation of equation 5. As is evident from equations 1-10 the parameters $\alpha_H$ and $\alpha_L$ become significantly more complex with increasing filter elements. The second parameter, the settling time (in this work the 2% settling time was chosen) may be approximated using equation 12 which is derived from the inverse laplacian of the system transfer function:

$$t_{2\%} = -\frac{1}{\alpha} ln\left[\frac{G(t)_{max}}{50}\right] \tag{12}$$

where α is the exponential power approximation of the impulse response decay. Consequently if the target function is defined as a function of the bandwidth ratio and settling time ratio as shown in equation 13:

$$H = \frac{\left(\beta_F / \beta_I\right)^n}{\left(t_F / t_I\right)^m} \tag{13}$$

where $n$ and $m$ are the power weightings given to each change, $\beta_F$ and $t_F$ are the bandwidth and settling time respectively of the modified system, $\beta_I$ and $t_I$ are the initial bandwidth and settling time respectively of the unmodified system. Then maximising this function, within realistic bounds, results in a good design for the four-tap equalisation filter. The system response with the maximised design may be seen in Figure 5. As may be observed there is an

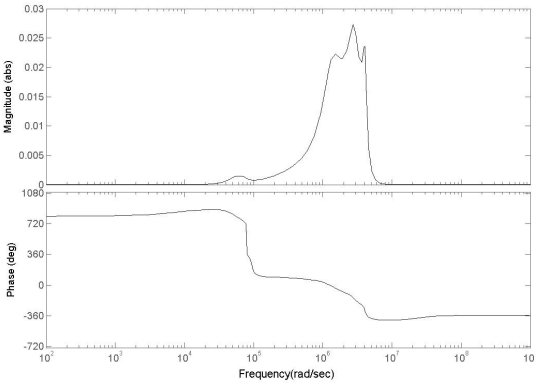


**Figure 5: Passive System Bode Response**

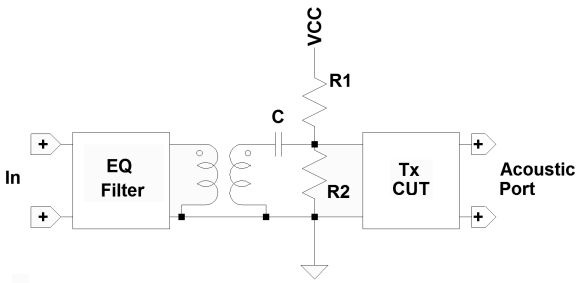


**Figure 6: Active Transmit Side Setup**

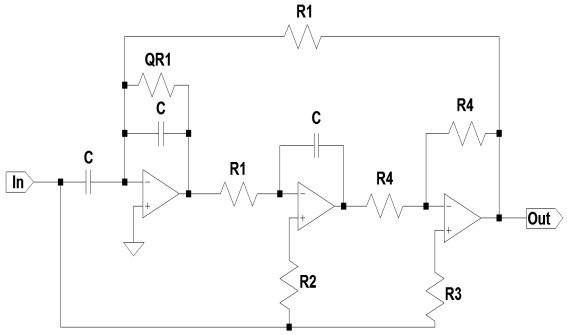


**Figure 7: Biquad All Pass Section**

increase in system 3dB bandwidth of 55% while the settling time has simultaneously been increased by only 28%. Although this represents only a four-tap filter, the approach may be scaled up to an arbitrary number of poles and zeros, the method of which is beyond the scope of this work.

*b) Op Amp Design*

The second design approach adopted is to use active equalisation filtering. This approach would be appropriate where pulsing is not used but rather pulse compression methods such as chirp signals. In this situation, a step up transformer is utilised as the transformed current draw by the transmitting CUT is nominal and well within most op amps capabilities. The transmit side equivalent circuit may be seen in Figure 6. As with the passive design a cascaded architecture was used for the equalisation filter. The design was restricted to four distinct biquadratic filtering elements, two all pass sections and two bandpass sections. Assuming that the transformer, in Figure 6 is ideal the load impedance on the driving side may be given by equation 14:

$$Z_L = \frac{-C_{mT} + C_{0T}(1 + C_{mT}s(R_{dT} + R_{rT} + L_{mT}s)}{\psi^2 C_{0T}^2 s(1 + C_{mT}s(R_{dT} + R_{rT} + L_{mT}s))} \qquad (14)$$

where $\psi$ is the transformer turns ratio and $C$ is the decoupling capacitance as shown in Figure 6. Phase equalisation was achieved using a second order Tow Thomas biquadratic section whose architecture may

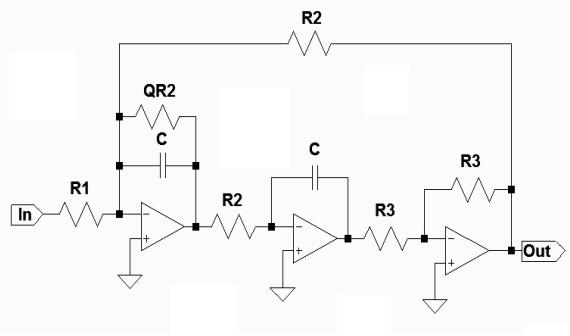


**Figure 8: Biquad Band Pass Section**

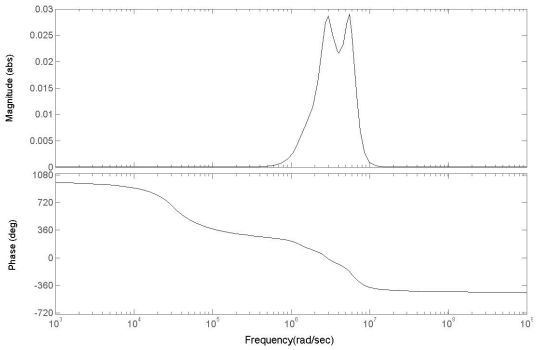


**Figure 9: Active System Bode Diagram**

be seen in Figure 7. The transfer function of a single all pass section may be given by equation 15:

$$G_{AP} = \frac{s^2\left(C_i/C\right) - s\left(R_4/CR_1R_3\right) + 1/C^2R_1R_2}{s^2 + s\left(1/QCR_1\right) + 1/C^2R_1^2} \qquad (15)$$

where $R_1$, $R_2$, $R_3$, $R_4$, $C$ and $C_i$ are as shown in Figure 7 and $Q$ is the q-factor of the filter. A biquadratic architecture was again used for the gain equalisation of the system response,. The design used may be seen in Figure 8. The transfer function of this section is given by equation 16:

$$G_{AP} = \frac{s\left(1/CR_2\right)}{s^2 + s\left(1/QCR_1\right) + 1/C^2R_1^2} \qquad (16)$$

where $R_1$, $R_2$ and $C$ are as shown in Figure 8. The overall system transfer function may be defined again as the product of the individual transfer functions and the 3dB bandwidth and settling time may be obtained in the same manner as defined previously. The optimised active system bode response may be seen in Figure 9. Maximising the relation defined in equation 14 for the active design resulted in a simulated bandwidth gain of 104% while settling time was decreased by 13%. The time domain impulse responses of the original system, the

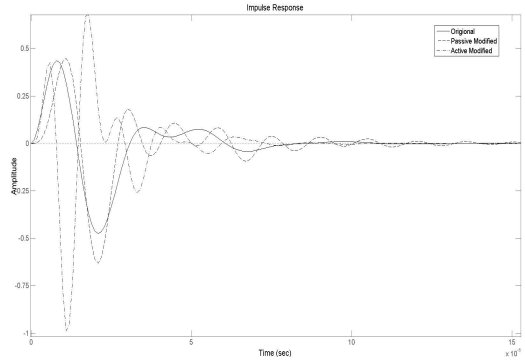


**Figure 10: System Impulse Responses**

passively equalised system and the actively equalised system can be seen in Figure 10. As is evident the shape of the impulse response is significantly affected by the equalisation with the active design being the most dramatically modified which is expected as the active system has the greatest coefficients in its transfer function. Future work will include correlating this impulse response data to experimental results.

## V CONCLUSIONS

It has been shown that the bandwidth, and the settling time of an ultrasonic through transmission system can be modified significantly through the use of simple equalisation networks in devices that do not operate with signal magnitudes in the order of dielectric breakdown. This includes a large subset of ultrasonic devices including receiver and SPL (sound pressure level) limited transmitter devices. An increase in centre frequency of 40% and 3dB bandwidth increase of 55% using a passive equalisation network were shown to be theoretically achievable with a through transmission system. In order to achieve these gains it has been shown that an increase of 28% in settling time was required. Additionally, an increase in centre frequency of 118% and 3dB bandwidth of 104% while simultaneously reducing settling time by 13% using an active filtering network were shown to be theoretically achievable.

Any configuration of through transmission ultrasonic system can be handled by this method as long as an accurate equivalent circuit model is available. As mentioned previously converging on a solution will become increasingly difficult with higher order composite filters. Future work will deal with developing the basic principles as presented in this work to more complicated equalisation architectures.

## REFERENCES


[1] M. Rafiq and C. Wykes "The Performance of Capacitive Ultrasonic Transducers Using V-Grooved Backplates" Meas. Sci. Technol. 2 , 1991, pp. 168-174

[2] D. W. Schindel, D. A. Hutchins, L. Zou and M. Sayer "The design and characterization of micromachined air-coupled capacitance transducers" IEEE Trans.Ultrason., Ferroelec., Freq. Contr., Vol. 42, No. 1, January 1995, pp.42-50

[3] A. Gachagan, G. Hayward, S. P. Kelly, and W. Galbraith "Characterization of Air Coupled Transducers" IEEE Trans.Ultrason., Ferroelec., Freq. Contr., Vol. 43, No. 4, July 1996 pp. 678-689

[4] M. I. Haller and B. T. Khuri-Yakub, "A Surface Micromachined Electrostatic Ultrasonic Air Transducer," 1994 IEEE Ultrasonic Symposium, pp. 1241-1244

[5] J. S. McIntosh, D. A. Hutchins, D. R. Billson, T. J. Robertson, R. A. Noble and A.D. R. Jones, "The characterization of capacitive micromachined ultrasonic transducers in air" Ultrasonics, Vol 40, Issues 1-8, May 2002, Pages 477-483

[6] G. Caliano, A. Caronti, M. Baruzzi, A. Rubini, A. Iula, R. Carotenuto, M. Pappalardo, "PSpice modelling of capacitive microfabricated ultrasonic transducers," Ultrasonics 40, 2002, pp. 449-455

[7] P.-C. Eccardt, K. Niederer, T. Scheiter, C. Hierold "Surface Micromachined Ultrasonic Transducers in CMOS Technology" 1996 IEEE Ultrasonics Symposium pp. 959-962

[8] A. Ramos, J. L. San Emeterio and P. T. Sanz, "Improvement in Transient Piezoelectric Responses of NDE Transceivers Using Selective Damping and Tuning Networks," IEEE Trans.Ultrason., Ferroelec., Freq. Contr., Vol. 47, No. 4, July 2000, pp. 826-835

[9] Zobel, O. J., "Theory and Design of Uniform and Composite Electric Wave Filters", Bell Systems Technical Journal, Vol. 2, pp. 1–46

[10] P. Mattila, F. Tsuzuki, H. Vaataja, and K. Sasaki, "Electroacoustic Model for Electrostatic Ultrasonic Transducers with V-Grooved Backplates", IEEE Trans.Ultrason., Ferroelec., Freq. Contr. Vol. 42. No. 1. January 1995, pp. 1-7

[11] Goksen G. Yaralioglu, Mohammed H. Badi, A. Sanli Ergun, and Butrus T. Khuri-Yakub, "Improved Equivalent Circuit and Finite Element Method Modeling of Capacitive Micromachined Ultrasonic Transducers", 2003 IEEE Ultrasonic Symposium, pp. 469-472

[12] Selim Olcum, Abdullah Atalar, Hayrettin K¨oymen and Muhammed N. Senlik, "Calculation of Transformer Ratio in Mason's Equivalent Circuit for cMUTs", 2006 IEEE Ultrasonic Symposium, pp. 1947-1950

[13] L. J. Bond, C. H. Chiang, and C. M. Fortunko, "Absorption of Ultrasonic Waves in Air at High Frequencies", Journal of the Acoustical Society of America, Vol 92, 1992, pp 2006-2015